Laboratory Observation of Resistive Electron Tearing in a Two-Fluid Reconnecting Current Sheet

Jonathan Jara-Almonte,* Hantao Ji, Masaaki Yamada, Jongsoo Yoo, and William Fox
Princeton Plasma Physics Laboratory, Princeton, New Jersey 08543, USA
(Received 4 April 2016; revised manuscript received 23 June 2016; published 25 August 2016)

The spontaneous formation of plasmoids via the resistive electron tearing of a reconnecting current sheet is observed in the laboratory. These experiments are performed during driven, antiparallel reconnection in the two-fluid regime within the Magnetic Reconnection Experiment. It is found that plasmoids are present even at a very low Lundquist number, and the number of plasmoids scales with both the current sheet aspect ratio and the Lundquist number. The reconnection electric field increases when plasmoids are formed, leading to an enhanced reconnection rate.

DOI: 10.1103/PhysRevLett.117.095001

Magnetic reconnection is a fundamental process in magnetized plasmas, wherein magnetic topology changes and magnetic energy is converted into particle energy [1]. A long-standing problem has been why the observed reconnection rate can be orders of magnitude faster than predicted by the classical fluid theory of Sweet [2] and Parker [3]. In an effort to address this problem, Hall effects have been invoked and shown to aid in fast reconnection when the ion inertial length ($c/\omega_{pi} = d_i$) exceeds the current sheet half-thickness (δ) [4,5]; however, this condition is not satisfied in many regimes of interest [6]. Only relatively recently has a plausible, but untested, explanation for fast reconnection in large, collisional systems appeared: the resistive plasmoid instability [7,8] of reconnecting current sheets.

The plasmoid instability breaks down elongated current sheets into multiple smaller current sheets separated by macroscopic magnetic islands (plasmoids). This breakdown typically is believed to occur via the tearing instability, which is destabilized at large Lundquist number $S = \mu_0 L V_A/\eta$ [7]. The resultant reconnection is typically unsteady, but the time-averaged rate is found to be enhanced and independent of resistivity [8]. The realization that resistive magnetohydrodynamics (MHD) allow for fast reconnection has spurred a renewed theoretical interest in both the tearing instability and fluid reconnection, e.g., [9–16].

Despite numerous theoretical works, there is limited experimental or *in situ* evidence for the destabilization of secondary tearing in collisional plasmas. Previous *in situ* observations and experiments have been limited to the regime of collisionless tearing either in nonreconnecting current sheets (i.e., primary tearing instead of secondary tearing) [17,18] or in actively reconnecting current sheets [19–21]. Remote sensing techniques cannot conclusively identify the magnetic field topology of plasmoids but have provided circumstantial evidence for collisional plasmoids on the Sun [22–24] and in laboratory fusion experiments [25]. In part, the lack of direct observations of collisional plasmoids is due to the large Lundquist numbers required for secondary tearing to occur within resistive MHD. In fact, new reconnection experiments are currently under construction with the primary goal of accessing the resistive plasmoid regime [6]. The theoretical predictions of a large critical Lundquist number are, however, untested.

In this Letter, we use the Magnetic Reconnection Experiment (MRX) [26] to study driven, quasisteady collisional reconnection, wherein we demonstrate secondary resistive tearing. Surprisingly, plasmoids are observed to form at Lundquist numbers well below resistive MHD predictions. The current sheets studied are formed during antiparallel reconnection in the two-fluid regime and are thinner than the ion inertial length yet thicker than both the electron inertial length and mean free path. Plasmoid formation is observed to be enhanced at higher Lundquist numbers. Finally, plasmoids are shown to be correlated with an enhancement of both the reconnection electric field and the normalized global reconnection rate. An examination of previous theoretical investigations suggests that electron-scale physics is responsible for plasmoid formation in this regime.

Figure 1(a) shows a schematic of the experiment. Plasma is produced via an inductive breakdown caused by pulsing the toroidal field coils located within the flux cores [26]. Reconnection is driven by ramping down the current in the poloidal field coils, such that the flux cores are a downstream sink of poloidal flux. Unlike previously reported experiments on MRX, the current setup includes four additional internal drive coils which provide an upstream source of poloidal flux.

For these experiments, the drive coils are critically important, as they extend the plasma regimes accessible in MRX to larger Lundquist numbers. Furthermore, by sourcing flux, the duration of quasisteady reconnection is prolonged, such that slowly growing instabilities can develop. The experiments presented here are well controlled and highly reproducible, allowing for the study of the

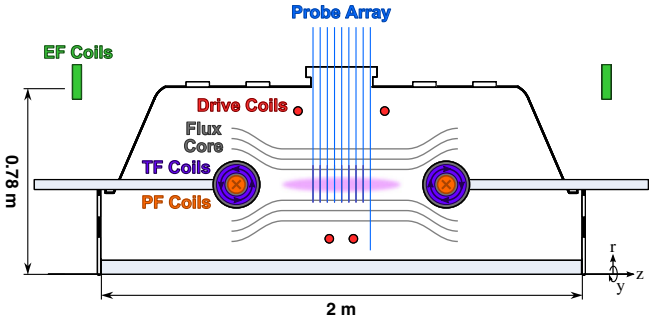

FIG. 1. Schematic of the Magnetic Reconnection Experiment showing the internal coils used to induce and drive reconnection, as well as the array of pickup coils used to measure the magnetic field. MRX is cylindrically symmetric, and the coordinate system used here is (r, y, z) corresponding to the inflow, out-of-plane, and outflow directions, respectively.

detailed dynamics of plasmoids and their consequences on the reconnection process. Here, the term plasmoid refers to 2D magnetic islands which are experimentally identified by searching for O points as described below.

These experiments are performed in collisional argon plasmas with initial neutral gas pressures of 1–4 mTorr. The typical plasma density and temperature are given by $n_e \approx 5 \times 10^{13}$ cm^{-3} and $T_e \approx 3$ eV upstream of the current sheet and $n_e \approx 2 \times 10^{14}$ cm^{-3} and $T_e \approx 4$ eV within the current sheet. As a result, these plasmas satisfy the length scale ordering $d_e \sim 0.5$ mm $< \lambda_{mfp} \sim 2$ mm $< \delta \sim 9$ mm $\ll d_i \sim 20$ cm, and so the measured plasma resistivity E_y/J_y is equal to the classical Spitzer resistivity $\eta_\perp$ (electron-neutral collisions are negligible) [27].

The main diagnostic used to characterize the current sheet is a large-scale 2D array of ~400 magnetic pickup coils measuring all three components of the magnetic field. The spatial resolution of the coils is nonuniform in order to optimally resolve both ion and electron scales, and the maximal resolution within the current sheet is 6 mm in the radial (r) direction and 3 cm in the axial (z) direction.

In order to positively identify the presence of plasmoids, we rely on multiple distinct analysis techniques. First, at a fixed time we infer the presence of poloidal nulls in the magnetic field via a direct interpolation between the closest magnetic coils. The classification of the detected nulls as either O points or X points is based on the local topology of the interpolated fields and is indicated via the green "X" and "O" symbols in Fig. 2.

As a secondary check, we have computed the Poincaré-Hopf index [28,29] of the poloidal magnetic field around suspected plasmoids and verified that it supports the results from direct interpolation. In this technique, the measured domain is split into 3 cm square cells, and the magnetic field is used to map the cell boundaries from a closed curve in configuration space (r, z) to a closed curve in the auxiliary space (B_r, B_z). The winding number about the origin in the auxiliary space is the Poincaré-Hopf index for that cell, and if it is nonzero, then the cell contains at least one null in the poloidal field [28].

Contours of the numerically integrated magnetic flux may also be used to identify large plasmoids; however, due to the inherent assumptions and limitations of the magnetic flux calculation, it has proven to be less reliable for identification of small plasmoids.

Finally, the time-dependent behavior has also been used to further validate the detection of plasmoids. The current sheet moves radially inwards as reconnection proceeds, and so the transit of a plasmoid can be directly observed on individual coils as a time-dependent reversal in the sign of the normal magnetic field (B_r) [19]. However, the current

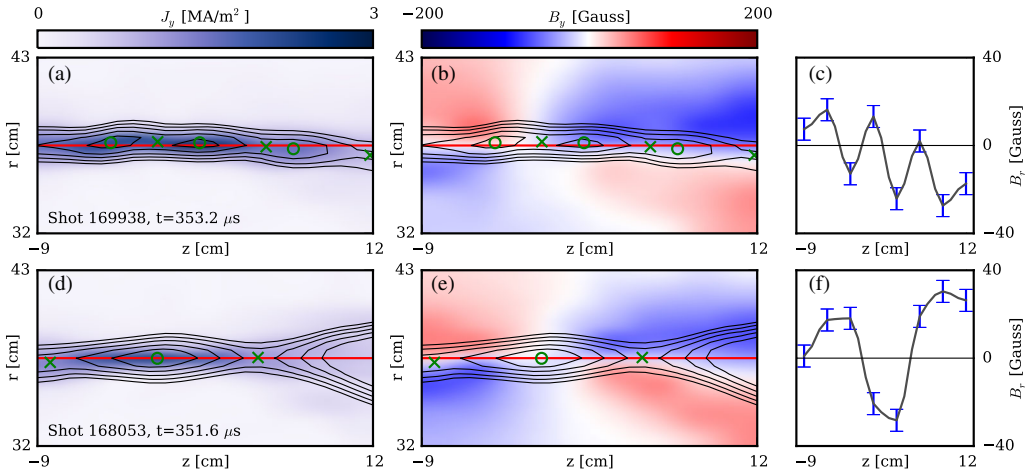

FIG. 2. Example discharges showing plasmoid formation either via a chain of small plasmoids [(a)–(c)] or via a single large plasmoid [(d)–(f)]. Contours of the poloidal flux and the locations of identified X points and O points are shown along with the out-of-plane current density (a),(d) and the out-of-plane Hall quadrupolar fields (b),(e). For clarity, flux contours outside of the central current sheet have been suppressed. (c),(f) The profile of the normal magnetic field B_r at $r = 37.5$ cm [red line in (a), (b), (d), and (e)], along with typical experimental uncertainties in the magnetic field measurement.

sheet motion is slow ($\lesssim$1 km/s), and so this technique is useful only for long-lived plasmoids.

Examples of typical plasmoid-unstable current sheets are shown in Fig. 2. Plasmoids are observed to form either as single, large plasmoids [e.g., Fig. 2(d)] or as a chain of small plasmoids [e.g., Fig. 2(a)]. As is evidenced by Figs. 2(b) and 2(e), despite being resistive and elongated, these current sheets are in the two-fluid regime, with pronounced Hall quadrupolar fields. For these plasmas, the electron inertial term is negligible, and so plasmoids are both embedded in a resistive current sheet and formed as the result of a resistive instability.

It is of primary interest to understand under what conditions plasmoids are formed. As a result of being resistive, the current sheet aspect is determined by the Lundquist number $S = \mu_0 L V_A/\eta$. For the experiments reported here, the magnetic field strength is varied while density is not, such that S alone is an appropriate dimensionless parameter by which to characterize the current sheet structure, as is demonstrated in Fig. 3(b), where the layer aspect ratio is observed to scale with the Lundquist number. Since the mass of argon is large, the Lundquist number achieved is small, $S < 100$, whereas incompressible resistive MHD simulations typically suggest that plasmoid formation does not occur until $S \gtrsim S_{\mathrm{crit}} \sim 10^4$ [8]. However, the underlying assumptions of incompressible resistive MHD are violated in these low β, large d_i plasmas, as will be discussed below.

In lieu of a comparison with the theory, the role of the current sheet structure on the formation of plasmoids is empirically examined. The average number of plasmoids present in the current sheet, $\langle n_O \rangle$, is defined to be the number of detected O points at any given instant [e.g., three in Fig. 2(a) and one in Fig. 2(d)], averaged over a time interval of 6.4 μs, comparable to the typical Alfvén time of 8.8 ± 3 μs. The interval is chosen once per discharge such that the current sheet is centered at $r = 37.5$ cm, where the spatial resolution is maximal. Figure 3(a) shows the observed scaling for the number of plasmoids. On average, more plasmoids are observed to form in a more elongated current sheet or, equivalently, at larger S. However, even at the largest values of S, not all current sheets are observed to form plasmoids. This, coupled with the relatively low aspect ratios, results in a low average number of observed plasmoids and is reflected in a large variance in the distribution of $\langle n_O \rangle$. Nonetheless, the mean behavior is well constrained due to the large number of discharges analyzed in this study.

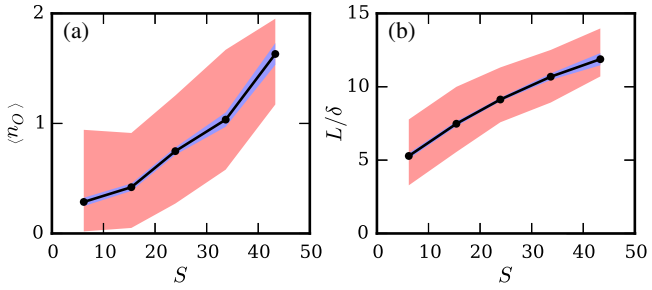

FIG. 3. (a) The observed time-averaged number of plasmoids $\langle n_O \rangle$ and (b) the current sheet aspect ratio versus the Lundquist number. The mean is given by the black line, whereas the red shaded region denotes the standard deviation, and the blue region is the standard error of the mean. On average, more plasmoids are seen in elongated, high S, current sheets.

This observed relationship between the number of plasmoids and the current sheet structure is qualitatively consistent with attributes of the canonical plasmoid instability, namely, that more elongated current sheets are more unstable, although the underlying tearing physics in these two-fluid current sheets is likely very different from that in resistive MHD.

One of the key predictions of the plasmoid instability theory is that the onset of plasmoids leads to higher global reconnection rates [8]. Since these experiments are already within the regime of two-fluid reconnection, the reconnection rate is fast (~0.1–0.2) even in the absence of plasmoids. Nonetheless, plasmoids can and do still affect the reconnection rate.

Experimentally, the reconnection electric field is determined from the time rate of change of the poloidal flux as evaluated at the dominant X point (i.e., the X point with the largest electric field). Figure 4 shows the time history of both the reconnection electric field and the number of observed plasmoids for a particular discharge. There is a clear correlation between the two; the formation of plasmoids corresponds to an enhancement of the reconnection electric field.

This enhancement is in fact routinely observed. Figure 5(a) shows the ensemble averaged time history of the reconnection electric field around a plasmoid formation event. At $\Delta t = 0$, a plasmoid is formed, and the electric field is immediately enhanced. Here, we define E_{t0} as the measured reconnection electric field just before a plasmoid is formed

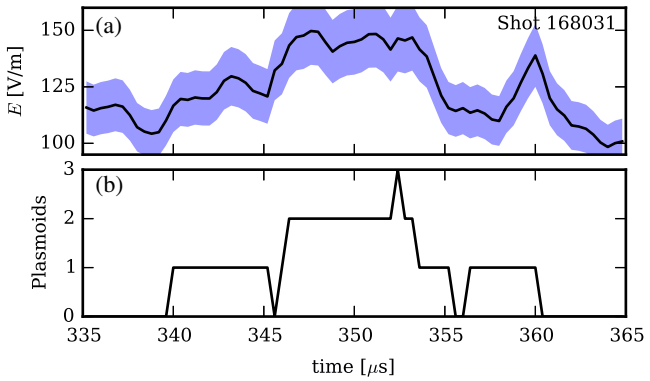

FIG. 4. Example of the correlation between plasmoids and enhancement of the reconnection electric field in a single discharge. The shaded region in (a) indicates a conservative estimate of 10% for the experimental uncertainty in the electric field measurement.

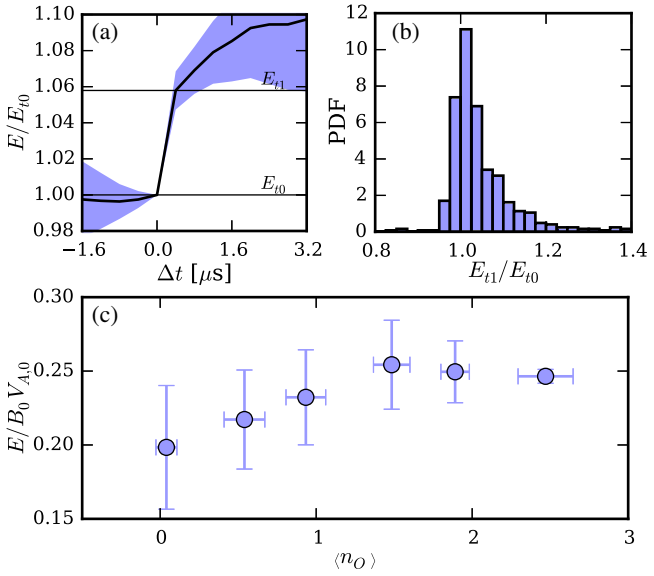

FIG. 5. Enhancement of the reconnection electric field during plasmoid formation. (a) Ensemble average of the time history of ~500 plasmoid formation events. The black line is the mean of all events, and the shaded region shows the standard error of the mean. (b) Statistically, more than 3/4 of events result in an increased electric field immediately after plasmoid formation, E_{t1}, relative to that before plasmoid formation, E_{t0}. (c) Relationship between the global reconnection rate and the number of plasmoids for 200 discharges. Error bars correspond to the standard deviation.

and E_{t1} as the electric field immediately afterwards. As shown in Fig. 5(b), E_{t1} is enhanced relative to E_{t0} in more than 3/4 of events. This enhancement is typically sustained over the plasmoid lifetime.

While an enhanced reconnection electric field implies faster flux transfer, the global reconnection rate is a normalized quantity conventionally defined as the ratio of the plasma inflow speed to the Alfvén velocity in the far upstream region where ideal MHD is valid. Using the ideal Ohm's law gives the relation $v_{in}/V_{A,0} = E/B_0V_{A,0}$, where the subscript 0 denotes upstream MHD quantities.

The reconnection electric field E is primarily determined by the local physics within the current sheet. In contrast, $B_0V_{A,0}$ is determined by the global properties of the system. As a result, plasmoid formation and dynamics in the two-fluid regime do not strongly affect $B_0V_{A,0}$; thus, plasmoids result in enhancements of both the reconnection electric field and the normalized reconnection rate. Figure 5(c) demonstrates this relationship. When one plasmoid is present on average, the normalized reconnection rate increases by ~10% in agreement with Fig. 5(a).

In summary, we have experimentally studied the formation of plasmoids in a collisional, sub-ion-scale current sheet. Plasmoids are identified using multiple distinct analysis techniques. The number of plasmoids is shown to scale with both the current sheet aspect ratio and the Lundquist number. It is suggested that the underlying mechanism for plasmoid formation is a two-fluid version of the canonical plasmoid instability, although a detailed confirmation requires full 2D eigenmode calculations including both compressibility and realistic equilibrium profiles. Such calculations are beyond the scope of the current work. Finally, the impact of plasmoids on the global reconnection rate is examined. It is found that the formation of plasmoids directly enhances the reconnection electric field. Since the global parameters are unaffected by plasmoids, the normalized global reconnection rate increases.

One of the major findings of this study is that resistive plasmoids can form even at Lundquist numbers which are predicted to be stable by the incompressible resistive MHD theory. However, previous theoretical analyses have shown that when nonideal effects, such as the Hall term [11,30], compressibility [12], or pressure anisotropy [31], are included, the growth rate of the resistive tearing instability can change dramatically, thereby changing the onset criterion of plasmoid instability. In particular, when Hall effects become important, electron physics dominate, and the tearing instability growth rate is independent of both ion and electron mass [32–35]. These analyses typically assume $S \gg 1$, $\delta > d_i$, and that density is uniform, thereby neglecting the influence of the equilibrium density profile, Hall quadrupolar field, and finite current sheet aspect ratio [35]. All of these effects are present in experiments, thereby motivating further theoretical developments. Fundamentally, the apparent discrepancy between these results and the resistive MHD theory is due to the introduction of electron-scale physics during two-fluid reconnection.

While the current study has focused solely on the physics of plasmoids, there exist a few interesting but unresolved questions. Typical Hall-MHD simulations [36] suggest that when $d_i > \delta$ the current sheet should spontaneously bifurcate to an X-shaped structure with $\delta \sim d_e = c/\omega_{pe}$ [4]. What are the physics behind the current sheet structure reported here where the relation $d_i \gg \delta \gg d_e$ is satisfied without an apparent X shape? How does it relate to the previously predicted intermediate, but unstable, equilibrium state in Hall-MHD [37]? Future work is warranted to address both of these questions as well as to understand 3D plasmoid and flux-rope dynamics.

This work is supported by NASA under Agreements No. NNH15AB29I and No. NNH14AX631, as well as by the DOE under Contract No. DE-AC0209CH11466. The authors thank W. Daughton for helpful discussions regarding the structure of Hall-MHD current sheets, as well as R. Cutler for technical support.

*jjaraalm@pppl.gov

[1] M. Yamada, R. Kulsrud, and H. Ji, Rev. Mod. Phys. **82**, 603 (2010).

[2] P. A. Sweet, in *Electromagnetic Phenomena in Cosmical Physics*, IAU Symposium, Vol. 6, edited by B. Lehnert

(Cambridge University Press, Cambridge, England, 1958), p. 123.
[3] E. N. Parker, J. Geophys. Res. **62**, 509 (1957).
[4] J. Birn, J. F. Drake, M. A. Shay, B. N. Rogers, R. E. Denton, M. Hesse, M. Kuznetsova, Z. W. Ma, A. Bhattacharjee, A. Otto, and P. L. Pritchett, J. Geophys. Res. **106**, 3715 (2001).
[5] Y. Ren, M. Yamada, H. Ji, S. P. Gerhardt, and R. Kulsrud, Phys. Rev. Lett. **101**, 085003 (2008).
[6] H. Ji and W. Daughton, Phys. Plasmas **18**, 111207 (2011).
[7] N. F. Loureiro, A. A. Schekochihin, and S. C. Cowley, Phys. Plasmas **14**, 100703 (2007).
[8] A. Bhattacharjee, Y.-M. Huang, H. Yang, and B. Rogers, Phys. Plasmas **16**, 112102 (2009).
[9] R. Samtaney, N. F. Loureiro, D. A. Uzdensky, A. A. Schekochihin, and S. C. Cowley, Phys. Rev. Lett. **103**, 105004 (2009).
[10] D. A. Uzdensky, N. F. Loureiro, and A. A. Schekochihin, Phys. Rev. Lett. **105**, 235002 (2010).
[11] S. D. Baalrud, A. Bhattacharjee, Y.-M. Huang, and K. Germaschewski, Phys. Plasmas **18**, 092108 (2011).
[12] L. Ni, U. Ziegler, Y.-M. Huang, J. Lin, and Z. Mei, Phys. Plasmas **19**, 072902 (2012).
[13] R. L. Fermo, J. F. Drake, and M. Swisdak, Phys. Rev. Lett. **108**, 255005 (2012).
[14] F. Pucci and M. Velli, Astrophys. J. Lett. **780**, L19 (2014).
[15] A. Tenerani, A. F. Rappazzo, M. Velli, and F. Pucci, Astrophys. J. **801**, 145 (2015).
[16] N. F. Loureiro and D. A. Uzdensky, Plasma Phys. Controlled Fusion **58**, 014021 (2016).
[17] W. Gekelman and H. Pfister, Phys. Fluids **31**, 2017 (1988).
[18] W. Gekelman, H. Pfister, and J. R. Kan, J. Geophys. Res. **96**, 3829 (1991).
[19] L.-J. Chen, A. Bhattacharjee, P. A. Puhl-Quinn, H. Yang, N. Bessho, S. Imada, S. Muhlbachler, P. W. Daly, B. Lefebvre, Y. Khotyaintsev, A. Vaivads, A. Fazakerley, and E. Georgescu, Nat. Phys. **4**, 19 (2008).
[20] M. Øieroset, T. D. Phan, J. P. Eastwood, M. Fujimoto, W. Daughton, M. A. Shay, V. Angelopoulos, F. S. Mozer, J. P. McFadden, D. E. Larson, and K.-H. Glassmeier, Phys. Rev. Lett. **107**, 165007 (2011).
[21] S. Dorfman, H. Ji, M. Yamada, J. Yoo, E. Lawrence, C. Myers, and T. D. Tharp, Geophys. Res. Lett. **40**, 233 (2013).
[22] K. Shibata and S. Tanuma, Earth, Planets Space **53**, 473 (2001).
[23] L.-J. Guo, A. Bhattacharjee, and Y.-M. Huang, Astrophys. J. Lett. **771**, L14 (2013).
[24] D. E. Innes, L.-J. Guo, Y.-M. Huang, and A. Bhattacharjee, Astrophys. J. **813**, 86 (2015).
[25] F. Ebrahimi and R. Raman, Phys. Rev. Lett. **114**, 205003 (2015).
[26] M. Yamada, H. Ji, S. Hsu, T. Carter, R. Kulsrud, N. Bretz, F. Jobes, Y. Ono, and F. Perkins, Phys. Plasmas **4**, 1936 (1997).
[27] A. Kuritsyn, M. Yamada, S. Gerhardt, H. Ji, R. Kulsrud, and Y. Ren, Phys. Plasmas **13**, 055703 (2006).
[28] J. M. Greene, J. Comput. Phys. **98**, 194 (1992).
[29] C. J. Xiao, X. G. Wang, Z. Y. Pu, H. Zhao, J. X. Wang, Z. W. Ma, S. Y. Fu, M. G. Kivelson, Z. X. Liu, Q. G. Zong, K. H. Glassmeier, A. Balogh, A. Korth, H. Reme, and C. P. Escoubet, Nat. Phys. **2**, 478 (2006).
[30] T. Terasawa, Geophys. Res. Lett. **10**, 475 (1983).
[31] Y. Shi, L. C. Lee, and Z. F. Fu, J. Geophys. Res. **92**, 12171 (1987).
[32] J. F. Drake and Y. C. Lee, Phys. Fluids **20**, 1341 (1977).
[33] V. V. Mirnov, C. C. Hegna, and S. C. Prager, Phys. Plasmas **11**, 4468 (2004).
[34] N. Bian and G. Vekstein, Phys. Plasmas **14**, 072107 (2007).
[35] E. Ahedo and J. J. Ramos, Phys. Plasmas **19**, 072519 (2012).
[36] Z. W. Ma and A. Bhattacharjee, J. Geophys. Res. **106**, 3773 (2001).
[37] P. A. Cassak, J. F. Drake, M. A. Shay, and B. Eckhardt, Phys. Rev. Lett. **98**, 215001 (2007).